

## Reversal of Step Roughness on Ge-Covered Vicinal Si(001)

Fang Wu, Xun Chen, Zhenyu Zhang, and M. G. Lagally

University of Wisconsin, Madison, Wisconsin 53706

(Received 4 February 1994)

The influence of Ge on the equilibrium step morphologies of vicinal Si(001) has been investigated quantitatively using scanning tunneling microscopy. As the Ge coverage  $\theta_{\text{Ge}}$  increases, the relative roughness of the two types of steps on the surface *reverses*. Physically, the accompanying evolving ( $2 \times n$ ) reconstruction modifies the kink energetics by introducing a new type of kink, and confines step meandering. The energies associated with these new kinks and the dependence of the step energies on  $\theta_{\text{Ge}}$  are extracted.

PACS numbers: 68.35.Md, 68.35.Bs, 68.35.Dv

For obvious scientific and technological reasons, the physical properties of the Ge-Si interface have been studied extensively. Ge/Si is a model system for Stranski-Krastanov growth [1,2]. Ge/Si devices offer the hope of a range of new high-speed electronic devices. Control of the film morphology and electronic properties of Ge/Si layered structures depends on understanding the initial stages of interface formation. Ge deposition on Si(001) serves as a model system for investigation of mechanisms controlling this interface formation. On clean Si(001) the top-layer atoms dimerize, leading to the  $2 \times 1$  reconstruction [3,4]. As Ge is deposited the surface reconstructs to form a ( $2 \times n$ ) structure [5,6]. Aspects of the interaction of Ge with a flat Si(001) surface that have been investigated include Ge-Si intermixing [7–9] and the influence of dimer vacancies on the stress field [10]. The presence of steps can play an important role in determining the interface morphologies in films subsequently grown on the substrate, as evidenced by recent growth studies of  $\text{Si}_x\text{Ge}_{1-x}$  alloys on vicinal Si(001) surfaces [11]. Most previous studies of the Ge/Si system have been carried out in regimes far from equilibrium, with relatively little attention paid to the structural properties of the interface in thermal equilibrium. In particular, no atomic-scale information is available on how the equilibrium step morphologies evolve as the Ge coverage increases, or on how Ge affects the free energy of the steps.

In this Letter, we present quantitative studies of the interaction of Ge adatoms with a vicinal Si(001) surface, focusing on the *thermal equilibrium* properties of the system. When Si(001) is miscut at small angles with the normal tilted towards the [110] direction, two types of monatomic-height steps form. The smooth  $S_A$  step is parallel to the upper-terrace dimer rows of the ( $2 \times 1$ ) reconstruction, while the rough  $S_B$  step is perpendicular to them. We show that Ge adsorption drastically changes the morphologies of both types of steps. The originally straight  $S_A$  step roughens as the Ge coverage  $\theta_{\text{Ge}}$  increases. The  $S_B$  step, which is originally rough, becomes increasingly straight. They become equally rough around  $\theta_{\text{Ge}} \sim 0.8$  ML, above which the original relative step roughness is *reversed*. We further show that there exists an intrinsic connection between the

crossover process in relative step roughness and the ordering of the ( $2 \times n$ ) reconstruction on terraces. The ( $2 \times n$ ) reconstruction introduces a new type of kink along the  $S_A$  steps; it also confines the meandering of the  $S_B$  steps as a result of step-vacancy interaction. Ge-Si bonds additionally modify the kink energies. The combined effect leads to the reversal of the relative step roughness as the Ge coverage increases.

The experiments were carried out in a UHV chamber equipped with a scanning tunneling microscope (STM) and a Ge deposition source. After initial thermal cleaning, the vicinal Si sample is annealed at  $600^\circ\text{C}$  for 5 min to allow equilibration of the clean Si(001) surface structure. Ge is then deposited at  $600^\circ\text{C}$ . After deposition the sample is annealed at  $600^\circ\text{C}$  for at least 1 h. It is then cooled and transferred to STM for imaging.

Figure 1 shows the principal observation of this work, the reversal of the step roughness induced by Ge adsorption on vicinal Si(001). Figure 1(a) is an STM image of the clean Si(001) surface miscut  $0.3^\circ$  toward [110]; the smooth  $S_A$  and rough  $S_B$  steps are clearly distinguishable. A step is roughened through the formation of kinks. A kink is defined by the sequential occurrence of two corners of opposite sense. Just as a step may have any height, a kink may have any length: The straight section between the corners defines the length of the kink. As Ge atoms are deposited onto the Si surface, the equilibrium step morphologies change in opposite directions: The  $S_B$  steps become smoother and the  $S_A$  steps rougher. At  $\theta_{\text{Ge}} \sim 0.8$  ML the two types of steps are visually equally rough [Fig. 1(b)]. Beyond this coverage the relative roughness is reversed. At  $\theta_{\text{Ge}} \sim 1.6$  ML, the  $S_B$  steps have become essentially straight except for a few long kinks, while the  $S_A$  steps are very rough [Fig. 1(c)]. The roughnesses exhibited in Figs. 1(a) and Fig. 1(c) are also qualitatively different, that in 1(c) being much more “jagged” or “boxy.” An STM image at higher resolution for  $\theta_{\text{Ge}} \sim 1.6$  ML is shown in Fig. 2. Here the dimer rows are clearly visible, confirming the identification of  $S_A$  and  $S_B$  steps.

The ( $2 \times n$ ) reconstruction, signaled by the dark dimer-vacancy (DV) lines, also is clearly observable in Fig. 2. The ( $2 \times n$ ) reconstruction is never perfect. Instead, the

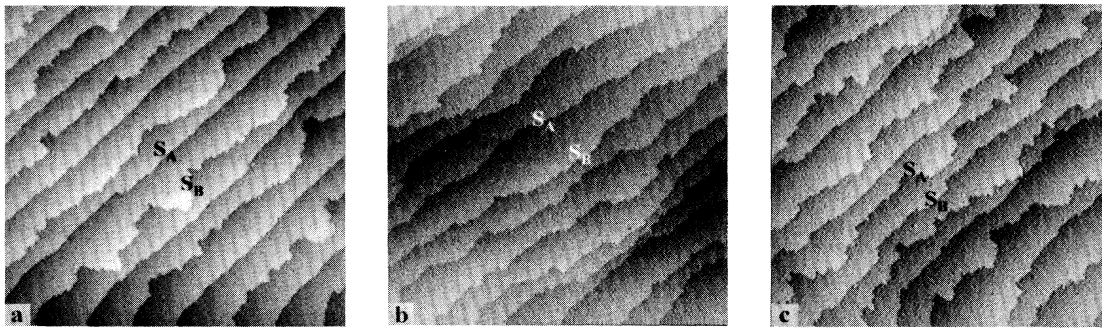


FIG. 1. STM images ( $3000 \text{ \AA} \times 3000 \text{ \AA}$ ) of vicinal Si(001) surface  $0.3^\circ$  miscut towards [110]. (a) Clean surface; (b) Ge-covered, with  $\theta_{\text{Ge}} \sim 0.8 \text{ ML}$ ; (c) Ge-covered, with  $\theta_{\text{Ge}} \sim 1.6 \text{ ML}$ . The two types of single-atomic-height steps  $S_A$  and  $S_B$  are denoted. The staircase is down from upper left to lower right.

value of  $n$ , the distance between adjacent missing dimers on the same dimer row, in units of the surface lattice constant  $a_0$ , follows a distribution function  $P(n)$ . Curve (a) in Fig. 3 shows that the measured  $P(n)$  for  $\theta_{\text{Ge}} \sim 0.8 \text{ ML}$ , peaked at  $n \sim 10$ , is a very broad distribution, indicating that the ordering of the  $(2 \times n)$  reconstruction is poor. As  $\theta_{\text{Ge}}$  increases, the dimer-vacancy concentration also increases. The intrinsic interaction [12] between the dimer vacancies drives them to line up with an average distance  $na_0$  between neighboring DV lines. At  $\theta_{\text{Ge}} \sim 1.6 \text{ ML}$ ,  $P(n)$ , with peak value shifted to  $n \sim 9$ , is much sharper [curve (b) in Fig. 3], indicating a better ordering of the  $(2 \times n)$  reconstruction. The degree of ordering scales with  $\theta_{\text{Ge}}$ , as measured by longer and better aligned DV lines, and is associated with stress changes on the surface [6,9,10].

The DV lines run across the terraces and terminate at the descending  $S_A$  steps, introducing a visually apparent new scale in units of  $na_0$ . In order to understand physically why the  $S_A$  and  $S_B$  steps change their morphologies as observed, it is desirable to carry out quantitative analysis

of the kink and step energetics as functions of the Ge coverage. For clean Si(001), such an analysis [13,14] explained why the  $S_B$  step is rough and the  $S_A$  step is smooth. A kink in the  $S_B$  step is just a segment of the  $S_A$  step; for a rough  $S_B$  step the total length of  $S_B$  segments is conserved, but the length of  $S_A$  segments increases as the step gets rougher. Conversely, a rougher  $S_A$  step introduces more  $S_B$  segments. At equilibrium the step free energy is minimized at a cost in step energy balanced by an increase in entropy. Because the energy per unit length of an  $S_A$  step is less than that of an  $S_B$  step, the cost in making  $S_A$  segments is less, and therefore the  $S_B$  step is rougher. In addition, there is a cost in corner energy, which is the same on both steps. For Ge-covered Si(001), however, a nontrivial modification of kink energy analysis is necessary to understand why the equilibrium step roughness for both types of steps is changed with increasing  $\theta_{\text{Ge}}$ . At finite  $\theta_{\text{Ge}}$ , the DV lines associated with the  $(2 \times n)$  reconstruction introduce two new features along the steps. First, along the  $S_A$  steps, kinks can form with much higher probability at the sites at which the DV lines terminate. Because of the difference in local bonding, these kinks have energies different from those at the normal sites, where there are no DV's. We differentiate them as vacancy-site (VS) kinks and normal-site (NS) kinks (Fig. 2). Second, since the DV

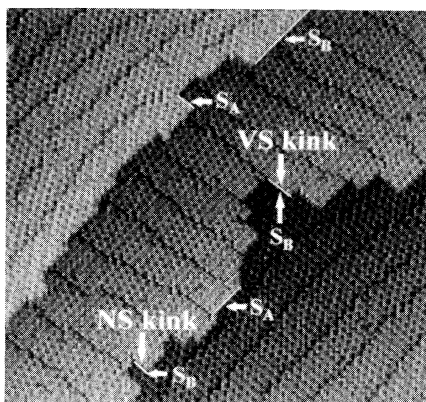


FIG. 2. STM image ( $450 \text{ \AA} \times 450 \text{ \AA}$ ) of Si(001) covered with  $\sim 1.6 \text{ ML}$  Ge, showing atomically resolved structures of steps, kinks, dimer-vacancy lines, and dimer rows perpendicular to these lines. Vacancy-site (VS) and normal-site (NS) kinks are shown along the  $S_A$  step. The figure also shows that a kink in the  $S_A$  step is just a section of the  $S_B$  step and vice versa.

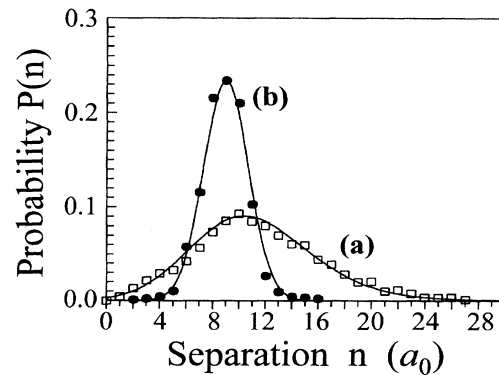


FIG. 3. The probability distribution  $P(n)$  of the separation  $n$  of two adjacent dimer-vacancy lines. (a)  $\theta_{\text{Ge}} \sim 0.8 \text{ ML}$ , (b)  $\theta_{\text{Ge}} \sim 1.6 \text{ ML}$ .

lines on the upper terrace are parallel to the  $S_B$  steps, they may limit the possible degree of the  $S_B$  step meandering. In addition, the existence of Ge creates Si-Ge and Ge-Ge bonds, which may alter the step energies.

In the following, we discuss the results for  $\theta_{\text{Ge}} \sim 1.6$  ML in more detail, in order to compare the step energetics for surfaces with roughness reversed from that of clean Si(001) [Figs. 1(a) and 1(c)]. For the  $S_A$  steps, we count the VS and NS kinks and analyze them separately. We have checked to make sure that the kinks for Ge-covered Si(001) are independent [as for clean Si(001)], i.e., no neighboring kink-kink correlation exists. When the kinks are independent, the number  $N(l)$  of kinks of length  $l$  must follow a Boltzmann distribution:  $N(l) \propto \exp[-E(l)/k_B T]$ , where  $E(l)$  is the excitation energy of kinks of length  $l$  and  $k_B T$  is the thermal energy. By plotting  $-\ln[N(l)/2N(0)]$  versus kink length  $l$ , we extract the kink energy as a function of kink length. The results for the  $S_A$  step are shown in Fig. 4(a) separately for VS and NS kinks. The data can be fitted with straight lines, i.e.,  $E_A(l) = l\epsilon_{SB} + C_A$ . They have the same slope,  $\epsilon_{SB}/k_B T = 0.62 \pm 0.06/(2a_0)$ , but different intercepts,  $C_{A,VS}/k_B T = 0.0 \pm 0.3$  and  $C_{A,NS}/k_B T = 2.0 \pm 0.3$ .

We now discuss the meaning and implications of these values. Because each NS and VS kink contains a section of  $S_B$  step, a single value  $\epsilon_{SB}$  for the  $S_B$  step energy per unit length  $2a_0$  is expected for both types of kinks. The difference in corner energies  $C_{A,VS}$  and  $C_{A,NS}$  results from the difference in local bonding at the inner corners of the two types of kinks: For every VS kink a dimer is missing at the inner corner, but this is not the case for a NS kink (Fig. 2). The value  $C_{A,VS} \sim 0.0$  implies a near-complete relaxation at the inner corner of a VS kink. The lower overall energy  $E_A(l)$  at the vacancy sites also indicates a higher kink excitation probability at these sites relative to that at normal sites. In other words, we expect to see kinks at the termination sites of the DV lines on the  $S_A$  steps. As  $\theta_{\text{Ge}}$  increases, the number of DV lines increases, providing more VS kinks and thus greater opportunity for the  $S_A$  step to develop the new type of roughness.

On a strained surface, the step energy contains mainly two contributions. One is positive and local, resulting from bond suppression and stretching along the step. The other is negative and nonlocal, resulting from the relief of the surface strain energy due to the creation of the step. Qualitatively, each of the two contributions leads to a monotonic decrease in the step energy as the Ge concentration is increased in the topmost layers. First, because the strength of a Ge-Ge bond or a Ge-Si bond is weaker than that of a Si-Si bond [8], an overall smaller step energy is expected as Si-Si bonds are replaced by Ge-Ge or Ge-Si bonds. Second, at higher  $\theta_{\text{Ge}}$ , the surface is more strongly strained, and the elastic energy released by the creation of a step is larger, producing an increasingly negative second term that reduces the magnitude of the step energy. The joint effect of both accounts for the observed decrease in  $\epsilon_{SB}$ . These argu-

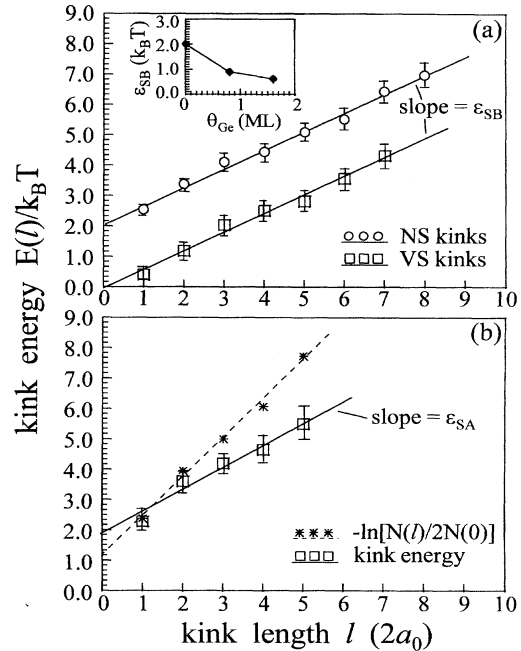


FIG. 4. Dependence of the kink energies on kink length for both types of steps, for  $\theta_{\text{Ge}} \sim 1.6$  ML. (a) Energies for VS and NS kinks of the  $S_A$  step. The data can be fitted by two straight lines, with the same slope  $\epsilon_{SB}$  and different intercepts. Note that a kink on the  $S_A$  step involves making segments of the  $S_B$  step (see Fig. 2). The inset figure shows that  $\epsilon_{SB}$  decreases as  $\theta_{\text{Ge}}$  increases. (b) Kink energy of the  $S_B$  step (squares), fitted by a solid line, whose slope is  $\epsilon_{SA}$ . The data are also plotted (stars), using a Boltzmann distribution with  $N(l)$  the total number of kinks of length  $l$ , together with a linear fit (dashed line).

ments should be true for both types of steps, although the magnitude of the effects may differ. The inset in Fig. 4(a) shows that the value of  $\epsilon_{SB}$  decreases as  $\theta_{\text{Ge}}$  increases.  $C_{A,VS}/k_B T$  and  $C_{A,NS}/k_B T$  do not change magnitudes for  $\theta_{\text{Ge}} \sim 0.8$  and 1.6 ML. The equilibrium temperature for this surface is estimated to be  $600 \pm 100$  K, giving  $\epsilon_{SB}(\theta_{\text{Ge}} \sim 1.6 \text{ ML}) = 32 \pm 5 \text{ meV}/(2a_0)$ . Because STM cannot yet differentiate between Ge and Si atoms, it is, at the moment, not possible to extract detailed information on the local atomic bonding geometry and the degree of Ge-Si intermixing on the surface [7] and hence to interpret the dependence of  $\epsilon_{SB}$  on  $\theta_{\text{Ge}}$  in more detail.

Next we shift our attention to the  $S_B$  steps, which are parallel to the DV lines on the upper terraces. We recall that the  $S_B$  steps become smoother with increasing  $\theta_{\text{Ge}}$ , implying that kinks become *harder* to create along these steps. It has been shown that the existence of the intrinsic vacancy-vacancy interactions on the Ge-covered Si(001)-(2 × n) surface leads to a strong confinement of the meandering of a given DV line by the presence of all the other DV lines [12]. Because an  $S_B$  step is essentially the same as a DV line judged from the point of view of the local bonding geometry, it is natural to expect this step

to be subjected to a confinement similar to that imposed on all the DV lines on terraces, forcing it to smoothen. In order to extract the intrinsic kink excitation energy from the meandering of the  $S_B$  steps, one must remove the effect of this confinement.

By analyzing the meandering of the  $S_B$  step, for  $\theta_{\text{Ge}} \sim 1.6$  ML, we find that the distribution function  $P_s(x)$  of its excursion  $x$  perpendicular to the step can be well fitted by a Gaussian (with width  $w \approx 2.6a_0$ ). A Gaussian distribution implies that the leading term of the effective confinement potential has a quadratic form  $V(l)/k_B T = (1/2)gl^2$ , where  $g$  is an effective force constant. In addition, we can show that the correlation between the meandering of the  $S_B$  step and its neighboring DV line is statistically negligible. Therefore, a mean-field approximation is applicable. The distribution of the kink lengths can then be solved exactly within the framework of the transfer matrix theory. The Hamiltonian contains two terms, the confinement potential  $V(l)$  and a term proportional to the kink excitation energy [12]. The true kink energy of the  $S_B$  step can be written

$$E_B(l)/k_B T = -\ln[N(l)/2N(0)] - \frac{1}{8}(g + w^{-2})l^2, \quad (1)$$

where the first term is just the usual Boltzmann distribution and the second term is the energy that describes the effect of the confinement. A plot ignoring the second term of Eq. (1) gives the stars in Fig. 4(b). A linear fit (dashed line) using  $E_B(l) = l\varepsilon_{SA} + C_B$  gives  $\varepsilon_{SA}/k_B T = 1.3 \pm 0.1/(2a_0)$ , a value almost 2 times that for clean Si(001) [13] that cannot be explained on physical grounds. The corner energy obtained in this way,  $C_B/k_B T = 1.2 \pm 0.3$ , is much smaller than  $C_{A,NS}/k_B T$ ; because the corners are identical, the values should be similar. These inconsistencies demonstrate the need to consider the confinement by vacancy lines, i.e., the complete Eq. (1). Given a trial value  $g$ ,  $E_B(l)$  can be obtained from Eq. (1). To determine the value of  $g$ , Metropolis Monte Carlo simulations were used to generate equilibrium kink configurations, from which the distribution  $P_s(x)$  is calculated and compared to the measured one until they converge. This procedure yields  $g \approx 0.04a_0^{-2}$ . The corresponding  $E_B(l)$  is plotted in Fig. 4(b) as squares. A linear fit (solid line) gives the true  $S_A$  step energy  $\varepsilon_{SA}/k_B T = 0.7 \pm 0.1/(2a_0)$ . The difference in the two lines in Fig. 4(b) [the second term in Eq. (1)] describes the contribution of the confinement energy, which makes long-kink formation more costly, leading to straightening of the  $S_B$  step. The similarity of the value of  $\varepsilon_{SA}$  to that for clean Si(001) [13], in contrast to the difference observed for  $\varepsilon_{SB}$ , suggests that the energy of an  $S_A$  step (along dimer rows) is less affected by Ge incorporation than is the energy of an  $S_B$  step (the end of dimer rows). The corner energy,  $C_B/k_B T = 1.8 \pm 0.4$ , now is within the error bar the same as  $C_{A,NS}/k_B T$  obtained above, as it should be. Thus, after consideration of con-

finement, physically reasonable values for step energies are obtained.

In conclusion, we have investigated the evolution of the equilibrium step morphology as a function of Ge coverage on vicinal Si(001). The originally straight  $S_A$  step roughens as the Ge coverage increases, while the  $S_B$  step, which is originally rough, becomes increasingly straight. At sufficiently high Ge coverages, the original relative roughness between the  $S_A$  and  $S_B$  steps is reversed. There exists an intimate connection between the variations in step morphology and development of the  $(2 \times n)$  reconstruction on terraces: The  $(2 \times n)$  reconstruction introduces a new type of kink along the  $S_A$  steps and confines the meandering of the  $S_B$  steps. From analysis of the step morphology it is possible to extract the dependence of step energy on Ge concentration and corner energies associated with structurally different kinks. This type of analysis can be generalized to other systems in which a reconstruction creates the possibility of new types of kinks and/or the confinement of steps.

This work was supported by NSF Materials Research Group Grant No. DMR91-21074 and by ONR.

- 
- [1] M. Asai, H. Ueba, and C. Tatsuyama, J. Appl. Phys. **58**, 2577 (1985); H.-J. Gossmann, L. C. Feldman, and W. M. Gibson, Surf. Sci. **155**, 413 (1985).
  - [2] D. J. Eaglesham and M. Cerullo, Phys. Rev. Lett. **64**, 1943 (1990).
  - [3] R. Schlier and H. Farnsworth, J. Chem. Phys. **30**, 917 (1959).
  - [4] R. M. Tromp, R. J. Hamers, and J. E. Demuth, Phys. Rev. Lett. **55**, 1303 (1985); Phys. Rev. B **24**, 5343 (1986).
  - [5] Y.-W. Mo and M. G. Lagally, J. Cryst. Growth **111**, 876 (1991).
  - [6] U. Köhler, O. Jusko, B. Müller, M. Horn-von Hoegen, and M. Pook, Ultramicroscopy **42-44**, 832 (1992).
  - [7] R. M. Tromp, Phys. Rev. B **47**, 7125 (1993).
  - [8] P. C. Weakliem and E. A. Carter, Phys. Rev. B **45**, 13 458 (1992).
  - [9] R. Butz and S. Kampers, Appl. Phys. Lett. **61**, 1307 (1992).
  - [10] J. Tersoff, Phys. Rev. B **45**, 8833 (1992).
  - [11] F. K. LeGoues, V. P. Kean, S. S. Iyer, J. Tersoff, and R. M. Tromp, Phys. Rev. Lett. **64**, 2038 (1990); D. E. Jesson, S. J. Pennycook, J.-M. Baribeau, and D. C. Houghton, Phys. Rev. Lett. **68**, 2062 (1992).
  - [12] Xun Chen, Fang Wu, Zhenyu Zhang, and M. G. Lagally, Phys. Rev. Lett. **73**, 850 (1994).
  - [13] B. S. Swartzentruber, Y.-W. Mo, R. Kariotis, M. G. Lagally, and M. B. Webb, Phys. Rev. Lett. **65**, 1913 (1990); B. S. Swartzentruber, Ph.D. thesis, University of Wisconsin-Madison, 1992 (unpublished).
  - [14] H. J. W. Zandvliet, H. B. Elswijk, E. J. van Loenen, and D. Dijkkamp, Phys. Rev. B **45**, 5965 (1992).

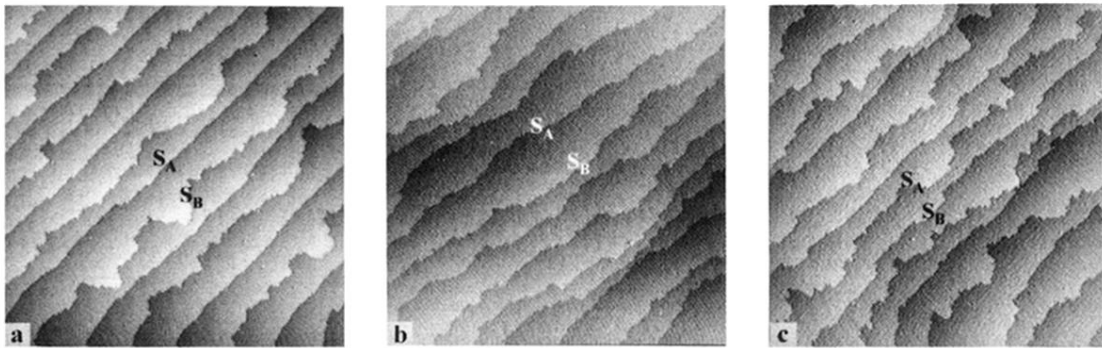


FIG. 1. STM images ( $3000 \text{ \AA} \times 3000 \text{ \AA}$ ) of vicinal Si(001) surface  $0.3^\circ$  miscut towards [110]. (a) Clean surface; (b) Ge-covered, with  $\theta_{\text{Ge}} \sim 0.8 \text{ ML}$ ; (c) Ge-covered, with  $\theta_{\text{Ge}} \sim 1.6 \text{ ML}$ . The two types of single-atomic-height steps  $S_A$  and  $S_B$  are denoted. The staircase is down from upper left to lower right.

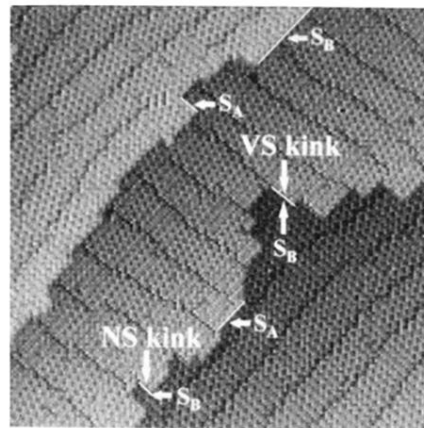


FIG. 2. STM image ( $450 \text{ \AA} \times 450 \text{ \AA}$ ) of Si(001) covered with  $\sim 1.6$  ML Ge, showing atomically resolved structures of steps, kinks, dimer-vacancy lines, and dimer rows perpendicular to these lines. Vacancy-site (VS) and normal-site (NS) kinks are shown along the  $S_A$  step. The figure also shows that a kink in the  $S_A$  step is just a section of the  $S_B$  step and vice versa.